Scattered Field Leapfrog ADI–FDTD Method for Drude Dispersive Media

Hasan K. Rouf and Daniel Erni

***Abstract*—This letter presents a new unconditionally stable scattered field (SF) finite-difference time-domain (FDTD) scheme for Drude dispersive medium based on leapfrog alternating direction implicit (ADI) technique. The proposed scheme introduces polarization current density and analytical incident field terms in the leapfrog scheme without adding extra computational complexities except causing minor changes in the coefficients for the central spatial locations. Unconditional stability and accuracy of the scheme are validated by numerical tests. When the Courant number is set to three or a higher value, the scheme can perform faster than the explicit FDTD scheme.**

***Index Terms*—Computational electromagnetics, Drude dispersive medium, finite-difference time domain (FDTD), scattered field techniques, unconditionally stable methods.**

I. Introduction

THE FINITE-DIFFERENCE time-domain (FDTD) problems can be solved by total field (TF) [1] or scattered field (SF) approaches [2]. In the SF approach, the incident field components are specified analytically throughout the problem space, while the scattered fields are found computationally. Incident and scattered fields must satisfy the Maxwell's equations independently. This approach can provide more accurate results when the scattered fields have much lower amplitudes than the total fields [2]. In the TF approach of FDTD formulation, incident and scattered field components are not separated. In this case, as the incident wave propagates through the grid, errors of such wave are progressively accumulated due to numerical dispersion and anisotropy. SF approach does not suffer from this limitation.

Unconditionally stable schemes like alternating direction implicit (ADI–)FDTD [3], [4] are not constrained by the Courant–Friedrich–Levy (CFL) stability criterion, and therefore significant computational advantage can be achieved. Recently, leapfrog ADI–FDTD method having the merit of not requiring mid-time computation, unlike ADI–FDTD, was proposed in [5]. Reference [6] analytically proved its stability and, by comparison among various unconditionally stable methods, showed that the one-step leapfrog ADI–FDTD method was the most efficient among all the recently developed unconditionally stable schemes. Despite many advantages of SF technique over TF technique, to our best knowledge, no SF unconditionally stable scheme has been developed so far. All the unconditionally stable schemes implemented TF formulation of the FDTD algorithm.

In this letter, a new scattered field unconditionally stable scheme is presented for Drude dispersive medium. The scheme is based on ADI principle but, unlike ADI, it does not require the splitting in two substeps. It follows the approach of [5], which presented the total field formulation for a frequency-independent medium. The scheme leads to one-step tridiagonal implicit equations that save both computational time and memory because, unlike ADI, no mid-time field computation and storage is required. We have adopted the auxiliary differential equation (ADE) method to incorporate Drude medium. Convolutional perfectly matched layer (CPML) [7] has been used to truncate the computational domain. The scheme has been validated against exact analytical solutions by numerical experiments. It is unconditionally stable beyond the CFL limit and can maintain very high accuracy even when the Courant number is quite high. The proposed scheme becomes computationally more efficient than the explicit FDTD when the Courant number equals or exceeds only three. Average relative errors at larger time-step sizes beyond the CFL limit have also been quantified.

II. Formulation

We consider a linear, isotropic Drude dispersive medium having the permittivity $\epsilon_{\rm r}(\omega) = \epsilon_\infty - \sum_{p=1}^{P} \frac{\omega_{\rm d,p}^2}{\omega^2 - j\omega\gamma_{\rm d,p}}$ [1], where $\omega_{\rm d,p}$ is the Drude pole frequency and $\gamma_{\rm d,p}$ is the inverse of the pole relaxation time. Now due to the linearity of Maxwell's equation, the total electric and magnetic fields can be expressed as the sum of incident and scattered fields. That is: $\boldsymbol{E}_{\rm tot} = \boldsymbol{E}_{\rm inc} + \boldsymbol{E}_{\rm scat}$ and $\boldsymbol{H}_{\rm tot} = \boldsymbol{H}_{\rm inc} + \boldsymbol{H}_{\rm scat}$. Here, $\boldsymbol{E}_{\rm inc}$ and $\boldsymbol{H}_{\rm inc}$ are the values of the incident wave fields, which are assumed to be known in the SF technique at all space points of FDTD grid and at all time-steps. $\boldsymbol{E}_{\rm scat}$ and $\boldsymbol{H}_{\rm scat}$ are the values of the scattered wave fields, which are initially unknown. These are fields that result from the interaction of the incident wave with any

Manuscript received September 13, 2015; revised December 22, 2015; accepted January 07, 2016. Date of publication January 12, 2016; date of current version September 02, 2016. This work was supported by the Alexander von Humboldt Foundation.

H. K. Rouf is with the Department of Applied Physics, Electronics and Communication Engineering, University of Chittagong, Chittagong 4331, Bangladesh, and also with the Department of General and Theoretical Electrical Engineering (ATE), Faculty of Engineering, University of Duisburg-Essen, and CENIDE—Center for Nanointegration Duisburg-Essen, 47048 Duisburg, Germany (e-mail: hasan.rouf@cu.ac.bd).

D. Erni is with the Department of General and Theoretical Electrical Engineering (ATE), Faculty of Engineering, University of Duisburg-Essen, and CENIDE—Center for Nanointegration Duisburg-Essen, 47048 Duisburg, Germany.

Color versions of one or more of the figures in this letter are available online at http://ieeexplore.ieee.org.

Digital Object Identifier 10.1109/LAWP.2016.2517572

materials in the grid. In the SF technique, the FDTD method is used to time-step only the scattered electric and magnetic fields. In the proposed algorithm, the incident field is specified to be propagating in free space for simplicity. Therefore, for the incident field in free-space, Faraday's law, $\nabla \times \boldsymbol{E} = -\mu \frac{\partial \boldsymbol{H}}{\partial t}$, is given by $\nabla \times \boldsymbol{E}_{\rm inc} = -\mu_0 \frac{\partial \boldsymbol{H}_{\rm inc}}{\partial t}$. For a dispersive medium, this equation is expressed as the total field: $\nabla \times \boldsymbol{E}_{\rm tot} = -\mu \frac{\partial \boldsymbol{H}_{\rm tot}}{\partial t}$. Taking $\mu \equiv \mu_0$ for nonmagnetized medium and subtracting the former equation from the latter, we obtain the scattered field expression

$$\nabla \times \boldsymbol{E}_{\rm scat} = -\mu \frac{\partial \boldsymbol{H}_{\rm scat}}{\partial t}. \tag{1}$$

Substitution of Drude permittivity in Ampère's law, $\nabla \times \boldsymbol{H} = \jmath\omega\epsilon_0\epsilon_{\rm r}(\omega)\boldsymbol{E}$, and conversion to time domain gives

$$\nabla \times \boldsymbol{H} = \epsilon_0\epsilon_\infty \frac{\partial \boldsymbol{E}}{\partial t} + \boldsymbol{J} \tag{2}$$

where the polarization current density $\boldsymbol{J}$ is found for a single-pole Drude medium as

$$\frac{\partial \boldsymbol{J}}{\partial t} + \gamma_{\rm d}\boldsymbol{J} = \epsilon_0\omega_{\rm d}^2\boldsymbol{E}. \tag{3}$$

Equation (2) can be written for an incident field in free space as $\nabla \times \boldsymbol{H}_{\rm inc} = \epsilon_0 \frac{\partial \boldsymbol{E}_{\rm inc}}{\partial t}$, and for a dispersive medium as $\nabla \times \boldsymbol{H}_{\rm tot} = \epsilon_0\epsilon_\infty \frac{\partial \boldsymbol{E}_{\rm tot}}{\partial t} + \boldsymbol{J}_{\rm tot}$. The scattered field expression for the propagating wave can be found by subtracting the former expression from the latter

$$\nabla \times \boldsymbol{H}_{\rm scat} = \epsilon_0\epsilon_\infty \frac{\partial \boldsymbol{E}_{\rm scat}}{\partial t} + \epsilon_0(\epsilon_\infty - 1)\frac{\partial \boldsymbol{E}_{\rm inc}}{\partial t} + \boldsymbol{J}_{\rm tot}. \tag{4}$$

In vector differential equations of (1) and (4), the incident fields are defined analytically. Updating equations for the scattered field components $\boldsymbol{E}_{\rm scat}$ and $\boldsymbol{H}_{\rm scat}$ are obtained using the proposed unconditionally stable scheme. According to the ADI principle, the time discretization from n to $n+1$ is split into two substeps: n to $n+1/2$ and $n+1/2$ to $n+1$. We start from this two-substeps procedure. From (4), considering the x-component of the electric field for the substep from n to $n+1/2$

$$\begin{aligned} E_{x,\rm scat}^{n+\frac{1}{2}} &= E_{x,\rm scat}^{n} + aD_yH_{z,\rm scat}^{n+\frac{1}{2}} - aD_zH_{y,\rm scat}^{n} \\ &\quad - c(E_{x,\rm inc}^{n+\frac{1}{2}} - E_{x,\rm inc}^{n}) - aJ_{x,\rm tot}^{n+m_1} \end{aligned} \tag{5}$$

where $a = \Delta t/2\epsilon_0\epsilon_\infty$, $c = (\epsilon_\infty - 1)/\epsilon_\infty$, $D_w = \partial/\partial w$ ($w = x, y, z$) and m_1 is the time index within the range of [0, 1/2]. Again from (1), considering the z-component of the magnetic field for the substep from n to $n+1/2$

$$H_{z,\rm scat}^{n+\frac{1}{2}} = H_{z,\rm scat}^{n} + bD_yE_{x,\rm scat}^{n+\frac{1}{2}} - bD_xE_{y,\rm scat}^{n} \tag{6}$$

where $b = \Delta t/2\mu$. Substituting (6) in (5)

$$\begin{aligned} (1 - abD_{2y})E_{x,\rm scat}^{n+\frac{1}{2}} &= E_{x,\rm scat}^{n} + a(D_yH_{z,\rm scat}^{n} - D_zH_{y,\rm scat}^{n}) \\ &\quad - abD_xD_yE_{y,\rm scat}^{n} \\ &\quad - c(E_{x,\rm inc}^{n+\frac{1}{2}} - E_{x,\rm inc}^{n}) - aJ_{x,\rm tot}^{n+m_1}. \end{aligned} \tag{7}$$

Next, $E_{x,\rm scat}$ from (4) is discretized from substep $n+1/2$ to $n+1$

$$\begin{aligned} E_{x,\rm scat}^{n+1} &= E_{x,\rm scat}^{n+\frac{1}{2}} + a(D_yH_{z,\rm scat}^{n+\frac{1}{2}} - D_zH_{y,\rm scat}^{n+1}) \\ &\quad - c(E_{x,\rm inc}^{n+1} - E_{x,\rm inc}^{n+\frac{1}{2}}) - aJ_{x,\rm tot}^{n+m_2} \end{aligned} \tag{8}$$

where m_2 is the time index within the range of [1/2, 1]. Again, discretizing $H_{z,\rm scat}$ in (1) from substep $n+1/2$ to $n+1$

$$H_{z,\rm scat}^{n+1} = H_{z,\rm scat}^{n+\frac{1}{2}} + b(D_yE_{x,\rm scat}^{n+\frac{1}{2}} - D_xE_{y,\rm scat}^{n+1}). \tag{9}$$

By substituting (9) in (8) and considering the previous time-step, we get

$$\begin{aligned} E_{x,\rm scat}^{n} &= E_{x,\rm scat}^{n-\frac{1}{2}} + a(D_yH_{z,\rm scat}^{n} - D_zH_{y,\rm scat}^{n}) \\ &\quad - ab(D_{2y}E_{x,\rm scat}^{n-\frac{1}{2}} + D_yD_xE_{y,\rm scat}^{n}) \\ &\quad - c(E_{x,\rm inc}^{n} - E_{x,\rm inc}^{n-\frac{1}{2}}) - aJ_{x,\rm tot}^{n+m_2-1}. \end{aligned} \tag{10}$$

Finally, we substitute (10) into (7) and, to avoid asymmetry error, set both m_1 and m_2 to 1/2 [8], which gives the expression of $E_{x,\rm scat}^{n+\frac{1}{2}}$ in terms of $J_{x,\rm tot}$ at current time-step

$$\begin{aligned} (1 - abD_{2y})E_{x,\rm scat}^{n+\frac{1}{2}} &= (1 - abD_{2y})E_{x,\rm scat}^{n-\frac{1}{2}} \\ &\quad + 2a(D_yH_{z,\rm scat}^{n} - D_zH_{y,\rm scat}^{n}) - c(E_{x,\rm inc}^{n+\frac{1}{2}} - E_{x,\rm inc}^{n-\frac{1}{2}}) \\ &\quad - a(J_{x,\rm tot}^{n+\frac{1}{2}} + J_{x,\rm tot}^{n-\frac{1}{2}}). \end{aligned} \tag{11}$$

$J_{x,\rm tot}^{n+\frac{1}{2}}$ is found from (3)

$$\begin{aligned} J_{x,\rm tot}^{n+\frac{1}{2}} &= \zeta J_{x,\rm tot}^{n-\frac{1}{2}} \\ &\quad + \eta(E_{x,\rm scat}^{n+\frac{1}{2}} + E_{x,\rm inc}^{n+\frac{1}{2}} + E_{x,\rm scat}^{n-\frac{1}{2}} + E_{x,\rm inc}^{n-\frac{1}{2}}) \end{aligned} \tag{12}$$

where $\zeta = \frac{2-\gamma_d\Delta t}{2+\gamma_d\Delta t}$ and $\eta = \frac{\epsilon_0\omega_d^2\Delta t}{2+\gamma_d\Delta t}$, and upon its substitution in (11), the final update equation for scattered electric field is obtained as

$$\begin{aligned} (1 + a\eta - abD_{2y})E_{x,\rm scat}^{n+\frac{1}{2}} &= (1 - a\eta - abD_{2y})E_{x,\rm scat}^{n-\frac{1}{2}} \\ &\quad + 2a(D_yH_{z,\rm scat}^{n} - D_zH_{y,\rm scat}^{n}) - (c + a\eta)E_{x,\rm inc}^{n+\frac{1}{2}} \\ &\quad + (c - a\eta)E_{x,\rm inc}^{n-\frac{1}{2}} - a(1 + \zeta)J_{x,\rm tot}^{n-\frac{1}{2}}. \end{aligned} \tag{13}$$

Equation (13) requires the solution of a tridiagonal matrix only once at a single time-step for calculating the scattered electric fields. Calculation and storage of fields at the intermediate time-step are not required. The presence of incident fields $E_{x,\rm inc}$ and polarization current density $J_{x,\rm tot}$ in (13) makes it different from the scheme presented in [5]. The former term stems from the implementation of scattered field technique, while the latter term results from the Drude dispersive medium. Due to the introduction of these terms, coefficients for central spatial locations ($E_{x,\rm scat}(i,j,k)$) are also altered. Thus, the scheme is implemented with no additional computational complexities.

The derivations for the magnetic fields are described now. From (5), using the corresponding expression for y-component of electric field, $E_{y,\rm scat}^{n}$ is obtained in the substep from n to $n+1/2$ and substituted in (6) to obtain $H_{z,\rm scat}^{n+\frac{1}{2}}$. Again in the

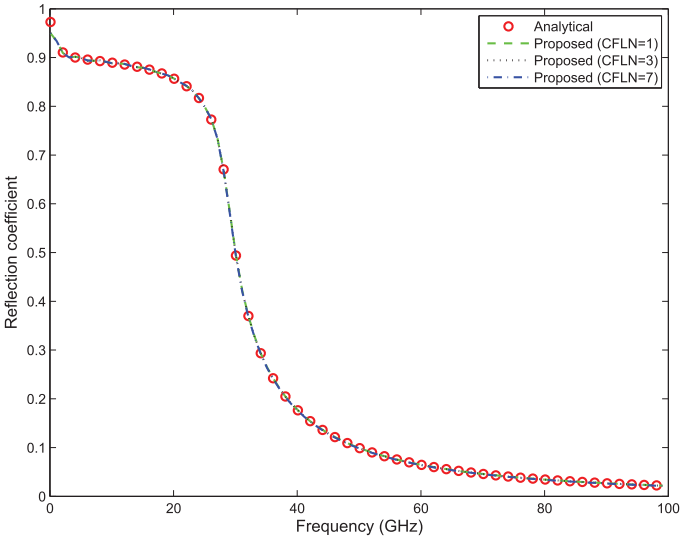

Fig. 1. Reflection coefficient at planar air–plasma interface computed by the proposed method at different CFLN and the analytical results (as reference).

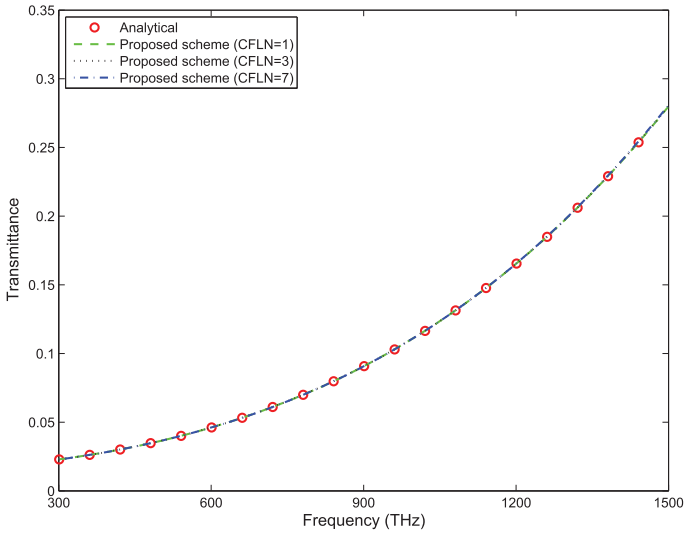

Fig. 2. Numerical and analytical values of transmittance of a 50-nm-thick gold slab.

substep from $n+1/2$ to $n+1$, $E_{y,\mathrm{scat}}^{n+1}$ is obtained similar to (8) and substituted in (9) to obtain $H_{z,\mathrm{scat}}^{n+1}$ in terms of $H_{z,\mathrm{scat}}^{n+\frac{1}{2}}$. Combining these two equations, both involving $H_{z,\mathrm{scat}}^{n+\frac{1}{2}}$, we get the final equation for calculating the magnetic fields as follows:

$$(1-abD_{2x})H_{z,\mathrm{scat}}^{n+1} = (1-abD_{2x})H_{z,\mathrm{scat}}^{n} + 2b(D_y E_{x,\mathrm{scat}}^{n+\frac{1}{2}} - D_x E_{y,\mathrm{scat}}^{n+\frac{1}{2}}). \quad (14)$$

Like the electric fields, calculation of the magnetic fields also requires the solution of a tridiagonal matrix at a single time-step. In summary, the complete procedure goes as follows:

- Solve (13) for the scattered electric fields.
- Solve (14) for the scattered magnetic fields.
- Find the polarization current density from (12).

III. Numerical Validation

The proposed scheme is validated by conducting two numerical tests and comparing the results to the analytical solutions. First, we considered an unmagnetized plasma characterized by Drude model having the parameters $\omega_\mathrm{d} = 2\pi \times 28.7$ GHz, $\gamma_\mathrm{d} = 2 \times 10^{10}$ GHz. We calculated the reflection coefficient when a plane wave is normally incident from air onto the plasma. In the numerical calculations, the grid size is $\Delta s = 29.98$ μm, and maximum time-step size allowed by the CFL limit is $\Delta t_{\mathrm{CFL}} = 10^{-13}$s. A modulated Gaussian pulse having significant spectral energy up to 100 GHz was used. Fig. 1 depicts the reflection coefficient calculated by the proposed scheme at different CFLN along with the analytical results. Here, the $\mathrm{CFLN} \equiv \Delta t/\Delta t_{\mathrm{CFL}}$, with Δt being the time discretization used in the simulation. The proposed scheme works even when $\mathrm{CFLN} > 1$, and the numerical results are in excellent agreement with the analytical values.

As a second example, we studied the transmission of light through a thin gold slab having the thickness of 50 nm. The thin gold slab is illuminated by a modulated Gaussian plane wave pulse with a spectral content up to 2000 THz. The cell size was 1 nm, and the dispersion of gold follows [9]: $\omega_\mathrm{d} = 11.96 \times 10^{15}$ rad/s, $\gamma_\mathrm{d} = 80.52 \times 10^{12}$ rad/s. Fig. 2 shows the transmittance of gold slab calculated by the proposed scheme at different CFLN together with the analytical solution. The proposed scheme provides an acceptable solution even for a large CFLN.

TABLE I
Comparison of the CPU Time and Average Relative Error

Method	CFLN	CPU time (s)	Average relative error
Explicit	1	39.719	
Proposed Method	1	76.078	0.00015813
Proposed Method	2	38.031	0.00050862
Proposed Method	3	25.531	0.0013
Proposed Method	4	19.203	0.0024
Proposed Method	5	15.281	0.0039
Proposed Method	7	10.812	0.0077

We then quantify the numerical error at higher CFLN by the average relative error $\mathcal{E}$ calculated over the whole frequency band: $\mathcal{E} = \sqrt{\sum_f (\mathcal{R} - \mathcal{R}^{\mathrm{ref}})^2 / \sum_f (\mathcal{R}^{\mathrm{ref}})^2}$. Here, $\mathcal{R}$ is the numerically calculated reflection coefficient, and $\mathcal{R}^{\mathrm{ref}}$ is the analytical reflection coefficient. For the numerical test of Fig. 2, the average relative errors of the proposed scheme at different CFLN are given in Table I. We see that the scheme can maintain good accuracy even at higher CFLN. For example, for $\mathrm{CFLN} = 1$, 3, and 7, the average relative errors are 0.0158%, 0.13%, and 0.77%, respectively. Table I also shows the CPU time required by the proposed scheme against the time required by the explicit FDTD method on the same computer. At $\mathrm{CFLN} = 3$, the proposed scheme becomes faster than the explicit scheme. At $\mathrm{CFLN} = 7$, the scheme becomes 3 times faster than the explicit scheme. By conducting several numerical tests, we found that the scheme renders beneficial in terms of computational speed when $\mathrm{CFLN} \geq 3$.

We further studied the robustness of the scheme by investigating its stability under more restrictive conditions. Reference

[10] showed that some of the popular auxiliary differential-equation-based explicit FDTD schemes associated with electromagnetic wave propagation in Drude medium are not stable when the plasma losses are deemed negligible (i.e., $\gamma_{\rm d} = 0$). To maintain stability, these schemes require $(\frac{\omega_{\rm d}\Delta t}{2})^2 << 1$, and $(\frac{\omega_{\rm d}\Delta t}{2})^2$ must not be equal to one. For such limiting cases (i.e., $\gamma_{\rm d} = 0$), we have set other parameters of the above numerical examples in such a way that makes $(\frac{\omega_{\rm d}\Delta t}{2})^2 \approx 1$ and studied the stability. For the first numerical example, we assumed the grid size to be $\Delta s = 299.8$ μm. If $\mathrm{CFLN} = 11$ and 12, then $(\frac{\omega_{\rm d}\Delta t}{2})^2 = 0.9836689$ and 1.170647, respectively. For the second numerical example with grid size $\Delta s = 4.99$ nm, setting $\mathrm{CFLN} = 10$ and 11 makes $(\frac{\omega_{\rm d}\Delta t}{2})^2 = 0.9933$ and 1.2019, respectively. Under all these restrictive conditions, the scheme always maintains its unconditional stability, which proves its robustness.

IV. Conclusion

A new unconditionally stable scattered field FDTD scheme has been developed for Drude dispersive medium. The scheme leads to tridiagonal implicit equations but, unlike ADI, it does not require the mid-time field computations. Numerical calculation of reflection coefficients at media interfaces and the transmittance of thin gold slab validated unconditional stability and accuracy of the scheme. The scheme can maintain very high accuracy even when the CFL limit is far exceeded. It becomes faster than the explicit FDTD scheme when the CFL number is as low as 3. Calculation of average relative errors showed that the scheme can maintain very high accuracy even beyond the Courant limit. The robustness of the scheme was established by conducting numerical tests in very restrictive conditions under which some other commonly used methods associated with Drude medium become unstable.

References

[1] A. Taflove and S. Hagness, *Computational Electrodynamics: The Finite-Difference Time-Domain Method*, 3rd ed., Boston, MA, USA: Artech House, 2005.

[2] K. Kunz and R. Luebbers, *The Finite Difference Time Domain Method for Electromagnetics*, Boca Raton, FL, USA: CRC Press, May 1993.

[3] T. Namiki, "A new FDTD algorithm based on alternating-direction implicit method," *IEEE Trans. Microw. Theory Tech.*, vol. 47, no. 10, pp. 2003–2007, Oct. 1999.

[4] F. Zheng, Z. Chen, and J. Zhang, "A finite difference time domain method without the Courant stability conditions," *IEEE Microw. Guided Wave Lett.*, vol. 9, no. 11, pp. 441–443, Nov. 1999.

[5] S. J. Cooke, M. Botton, T. M. Antonsen Jr., and B. Levush, "A leapfrog formulation of the 3D ADI-FDTD algorithm," *Int. J. Numer. Modeling, Electron. Netw., Devices Fields*, vol. 22, pp. 187–200, 2009.

[6] S. C. Yang, Z. Chen, and Y. Yu, W. Yin, "An unconditionally stable one-step arbitrary-order leapfrog ADI-FDTD method and its numerical properties," *IEEE Trans. Antennas Propag.*, vol. 60, no. 4, pp. 1995–2003, Apr. 2012.

[7] J. Roden and S. Gedney, "Convolution PML (CPML): An efficient FDTD implementation of the CFS-PML for arbitrary medium," *Microw. Opt. Technol. Lett.*, vol. 27, no. 5, pp. 334–339, 2000.

[8] B. Donderici and F. L. Teixeira, "Symmetric source implementation for the ADI-FDTD method," *IEEE Trans. Antennas Propag.*, vol. 53, no. 4, pp. 1562–1565, Apr. 2005.

[9] M. Okoniewski and E. Okoniewska, "Drude dispersion in ADE FDTD revisited," *Electron. Lett.*, vol. 42, no. 9, pp. 503–504, Apr. 27, 2006.

[10] J. L. Young and R. O. Nelson, "A summary and systematic analysis of FDTD algorithms for linearly dispersive media," *IEEE Antennas Propag. Mag.*, vol. 43, no. 1, pp. 61–77, Feb. 2001.